JOURNAL OF MATERIALS SCIENCE 27 (1992)2237–2242

Micro-Raman spectroscopy study of the process of microindentation in polymers

Part II *Poly(vinylidene fluoride)*

T. JAWHARI, J. C. MERINO, J. M. PASTOR
Departamento Física de la Materia Condensada, Universidad de Valladolid, 47011 Valladolid, Spain

The Raman analysis of the effect of pressures applied to poly(vinylidene fluoride) (PVF_2) samples shows a gradual crystalline transformation from structure II to I as the pressure is increased. This result was utilized to study the distribution of stress in the residual deformed micro-region produced by a process of microindentation in PVF_2 using a Vickers microhardness tester. The micro-Raman mapping of the microindented zone shows a gradual variation from form I to form II as the spectra were scanned from the centre to the edge of the impression area. This result indicates that the distribution of pressure is not constant in the micro-deformed zone, the stress being greater at the centre and decreasing as the edge of the residual impression is reached. The variation of stress was also determined for different loads and time of indentation.

1. Introduction

During the last fifteen years, the microhardness test has been used in the field of polymer science [1]. This technique, which consists of producing a microindentation at the surface of the material to be studied, provides valuable information on the resistance to deformation. The microhardness value of the material is then obtained by measuring the size of the impression. Because the dimensions of the deformed region are of the order of few tens of micrometres, the microhardness test is considered to be a non-destructive technique. Some works [2–5] have attempted to correlate the microhardness value with parameters that characterize the structure of semicrystalline polymers, that is crystallinity, lamellar thickness, chain orientation, etc. It was shown that this relatively simple technique is particularly sensitive to detect structural changes in the material [6–10]; for example, the value of the microhardness shows an important discontinuity at the glass temperature transition [7, 10], therefore the microhardness test can be used for rapid determination of weak second-order transitions. Although the microhardness technique has proved to be a rapid means of characterizing mechanical properties at the surface of polymers, it is still little used in the study of the relationship between microhardness and microstructure of polymers. The main reason is that the mechanisms of the process of microindentation in polymers are not well known. Although different models [11–13] have been proposed to describe the process of microindentation in elastoplastic materials such as metals, these may not be directly applied without precautions to polymeric materials because they show a viscoelastic behaviour. In addition, the behaviour of one polymer sample may differ greatly from that of another polymeric material, depending on the molecular weight, degree of crystallinity, thermal treatment, temperature, etc. Also, great care in the experimental analysis should be taken in order to obtain consistent microhardness data, because creep will generally occur during loading as well as time-dependent recovery when the load is retrieved.

In a previous work [14] we showed that the distribution of pressure in a microindentation produced in poly(3,3-dimethyl oxetane) may be achieved by following, at a molecular level, the crystalline transition from one structure to the other. Such a crystalline transition was found to be dependent on the stress applied to the sample, i.e. an increase in the applied pressure is characterized by an increase in the crystalline transformation from the orthorhombic to the monoclinic structure. This crystalline transformation was analysed by micro-Raman spectroscopy, and a mapping of the micro-region corresponding to the residual impression was given.

The aim of the present work was to continue the study of the process of microindentation in other polymeric materials with similar characteristics, i.e., showing structural changes with pressure, in order to observe possible differences in the response of the polymer to the applied stress. The material which was analysed in this work was PVF_2. It is well known that PVF_2 exhibits different crystalline structures that are sensitive to the stress submitted to the sample [15, 16]. This study will be particularly focused on the analysis of the variation of the degree of crystalline transformation along the indentation as a function of load,

0022–2461

time, etc., in order to obtain the distribution of residual stress in the microdeformed region.

2. Experimental procedure

2.1. Materials

PVF_2 is an important industrial polymeric material because of its ferroelectric properties. It was reported [15] that PVF_2 shows at least four different crystalline structures, depending on the sample preparation conditions: when PVF_2 is cooled from the melt to room temperature, the sample principally exhibits the crystalline form, II, which corresponds to the nonplanar TGTG′ conformation. The all-*trans* planar conformation of form I is produced by stretching the form II sample at room temperature. The other two crystal modifications (II_p and III) of PVF_2 can be obtained by solution casting, annealing, varying the rate of cooling, poling, etc. [16]. Form I is considered to be thermodynamically the most stable of the different crystalline structures, whereas form II is kinetically the most favourable.

In this study, a commercial PVF_2 sample (PVDF SOLEF-1012), was used. A 1 mm thick polymer plate was prepared by hot-pressing the PVF_2 pellets at 210° C and then cooled at room temperature. In order to correlate the crystalline transformation with the pressure submitted to PVF_2, a series of PVF_2 plates was obtained by pressing the initial polymer sample between 0 and 120 MPa for 1 min.

2.2. Testing procedures

A Vickers microhardness instrument (square pyramidal diamond indentor with an apical angle of 136°) combined with an optical universal Zeiss microscope was used during this work. The indentations were made at room temperature and the loads were applied for 1 min. The microhardness values were calculated by measuring the diagonal length of the permanent deformed area

$$MH_V = 2\sin 68° L/D^2 \quad (1)$$

where MH_V is the microhardness (MPa), L the applied load (N) and D the diagonal length of the indentation (mm).

The Raman instrument used was a multichannel detection (512 intensified diodes) Dilor XY spectrometer. The dispersive system of the instrument is constituted of a foremonochromator (a double monochromator) followed by a spectrograph. The Raman instrument was coupled to a standard Olympus microscope and the collection optics system utilized was the backscattering configuration. It was demonstrated in a previous study [14] that such a micro-Raman spectrometer allows Raman analysis of microsamples with a spatial resolution of the order of 1–2 μm. The excitation source was provided by a spectra Physics continuous argon-ion laser (model 2020/5w) emitting radiation at 514.5 nm. The laser power at the sample position was of the order of 10 mW. The spectra were recorded with a spectral bandpass of 150 μm. A time acquisition of 1 s was used and the number of scans was 50.

3. Results

The phase transition in PVF_2 from form II to form I can be well characterized by studying the changes occurring in the Raman spectrum. The two strongest bands present in the Raman spectrum of PVF_2 at 799 and 840 cm^{-1} were assigned to the nonplanar (TGTG′) conformation (Form II) and to the planar zigzag (TTTT) conformation (Form I), respectively

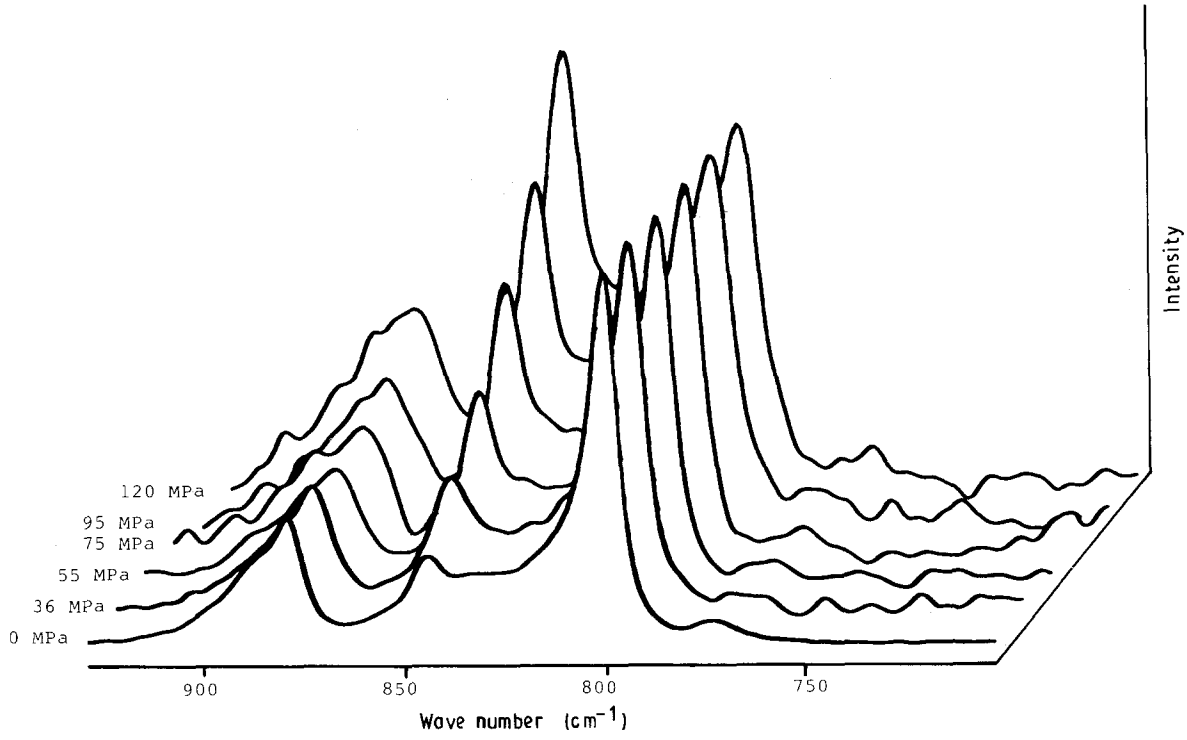

Figure 1 Raman spectra of PVF_2 recorded between 700 and 925 cm^{-1} for samples pressed between 0 and 120 MPa.

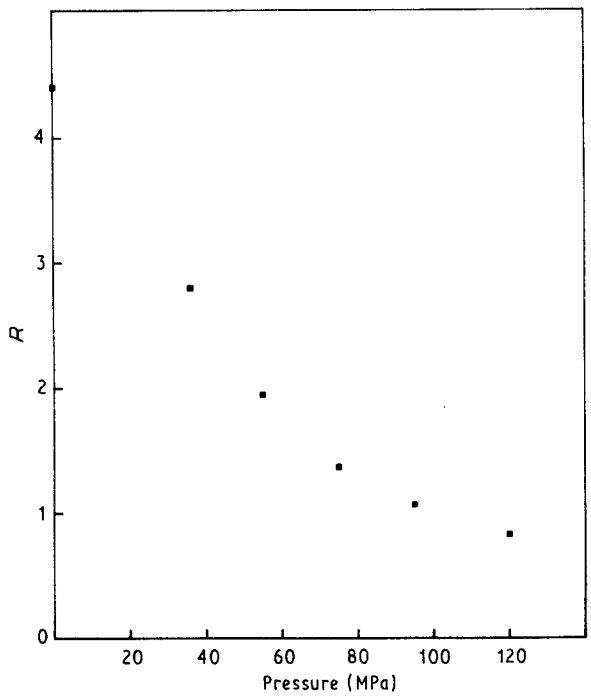

Figure 2 Peak intensity ratio $R = I_{799\ cm^{-1}}/I_{840\ cm^{-1}}$ calculated from the Raman spectra presented in Fig. 1, plotted against applied pressure.

[17–20]. These two bands were then chosen in this study to follow the crystalline phase transition in PVF_2 when the sample was submitted to a pressure. Fig. 1 shows the evolution of the Raman spectrum of PVF_2 between 700 and 925 cm^{-1} for samples pressed between 0 and 120 MPa. For a clearer visualization of the crystalline transformation, the peak intensity ratio $R = I(799\ cm^{-1})/I(840\ cm^{-1})$ is plotted in Fig. 2 versus the applied pressure.

A series of microindentations were produced on PVF_2 with different loads, i.e. 0.25, 0.50, 1.0, 1.5 and

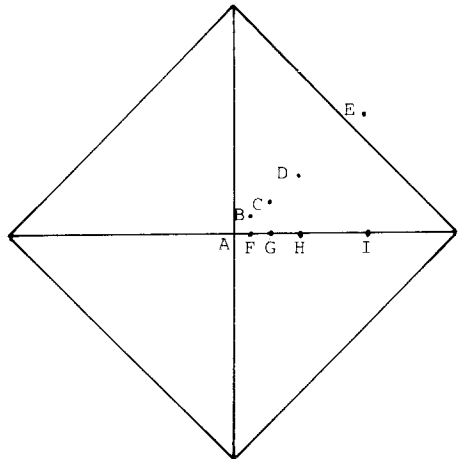

Figure 3 Schematic representation of the microindentation region (the diagonal length being equal to 77 μm) with the different positions where the Raman spectra were recorded, i.e., A (centre), B (2.5, 2.5 μm), C (5, 5 μm), D (10, 10 μm), E (20, 20 μm), F (0, 2.5 μm), G (0, 5 μm), H (0, 10 μm) and I (0, 20 μm).

2.0 N, applied for 1 min and analysed by Raman microspectroscopy along the line of maximum gradient in depth at the following positions: A (centre), B (2.5, 2.5 μm), C (5, 5 μm), D (10, 10 μm) and E (20, 20 μm), where the centre of the indentation is considered as the origin of the two axes formed by the diagonals of the indentation. Fig. 3 illustrates the different positions where the Raman spectra were recorded along the microindentation obtained with a load of 0.5 N. The diagonal length for these above microindentations was 55, 77, 110, 140 and 155 μm, respectively, which corresponds to a microhardness value of the order of 150 Mpa for each of them. To illustrate the variation of the Raman spectra along the microindentation, two of the five series of spectra are presented in Figs 4 and 5, which correspond to the

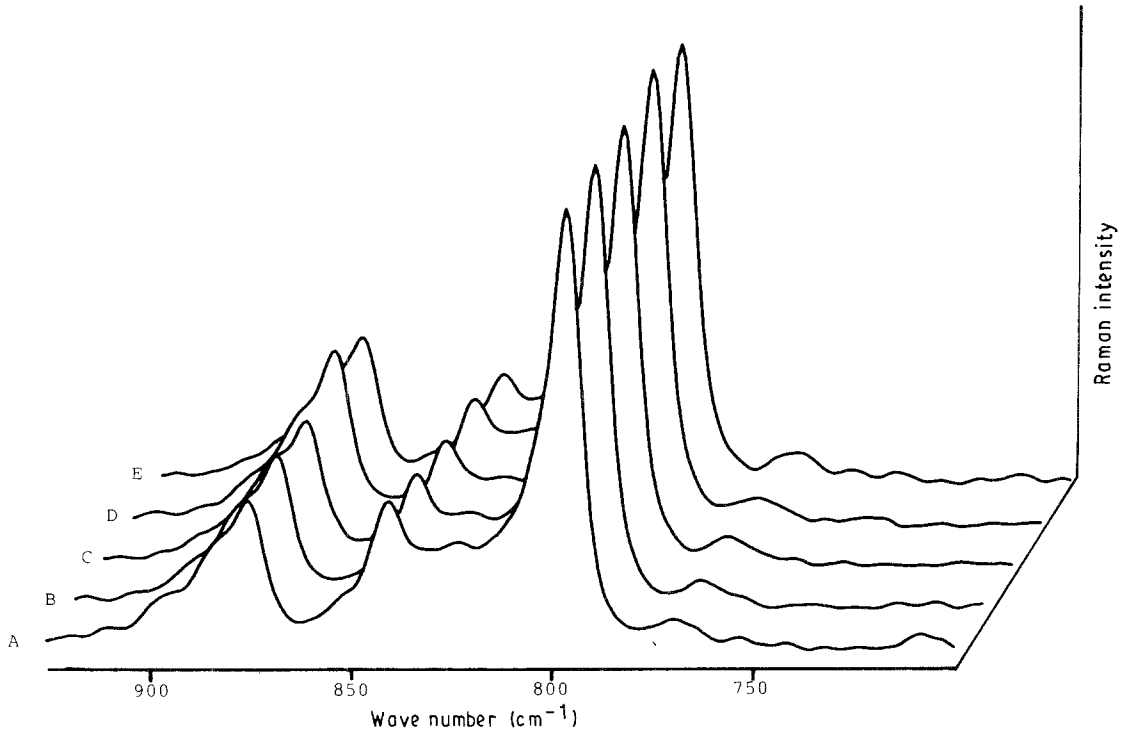

Figure 4 Raman spectra of PVF_2 recorded at the positions A, B, C, D and E for the microindentation obtained with a load of 0.5 N.

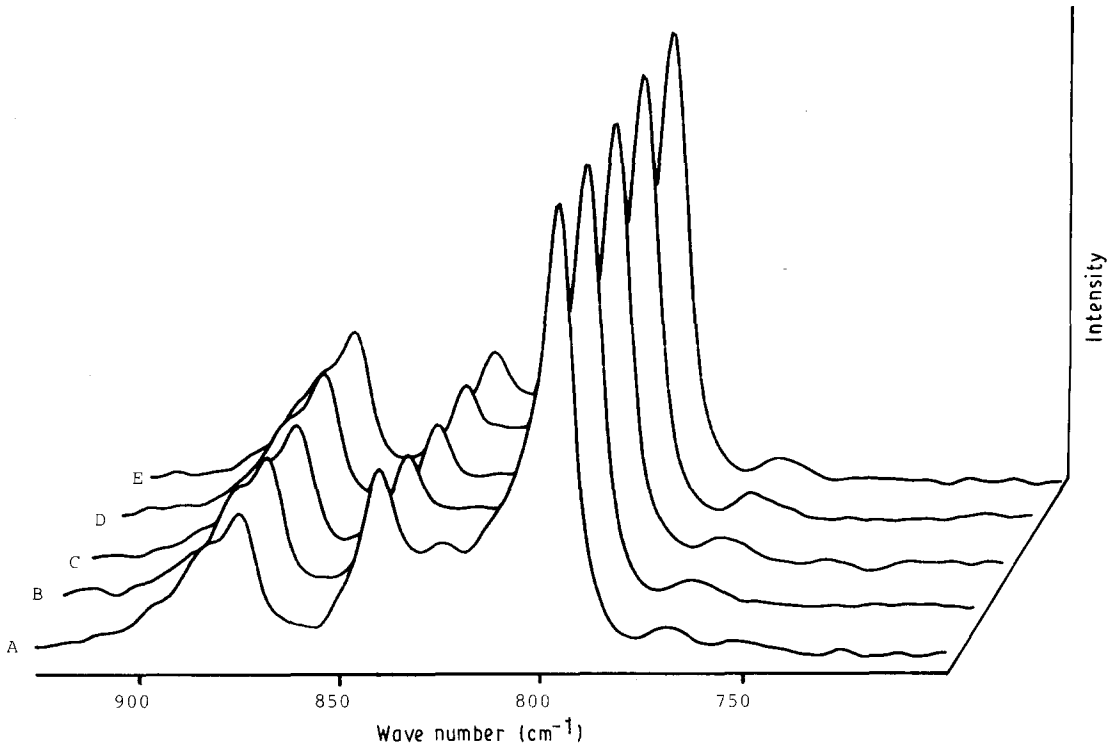

Figure 5 Raman spectra of PVF_2 recorded at the positions A, B, C, D, and E for the microindentation obtained with a load of 2 N.

microindentations obtained with a load of 0.5 and 2.0 N, respectively. The peak intensity ratio $R = I(799\ cm^{-1})/I(840\ cm^{-1})$ is plotted for each microindentation versus d, the distance between the centre of the impression and the position where the Raman spectrum was recorded. These plots are shown in Fig. 6. Fig. 7 shows the variation of the ratio R as a function of the applied load on the microindentor for spectra recorded at the centre of the impression.

A microindentation was also produced with a load of 2.0 N with instantaneous unloading of the indentor when the maximum load was reached. The Raman spectra were recorded at positions A, B, C, D and E and the resulting intensity ratios, R, are plotted against d in Fig. 8. The plot of Fig. 6 for the microindentation obtained with a load of 2.0 N (applied for 1 min) is also presented in Fig. 8 in order to compare the effect of the applied load time on the crystalline

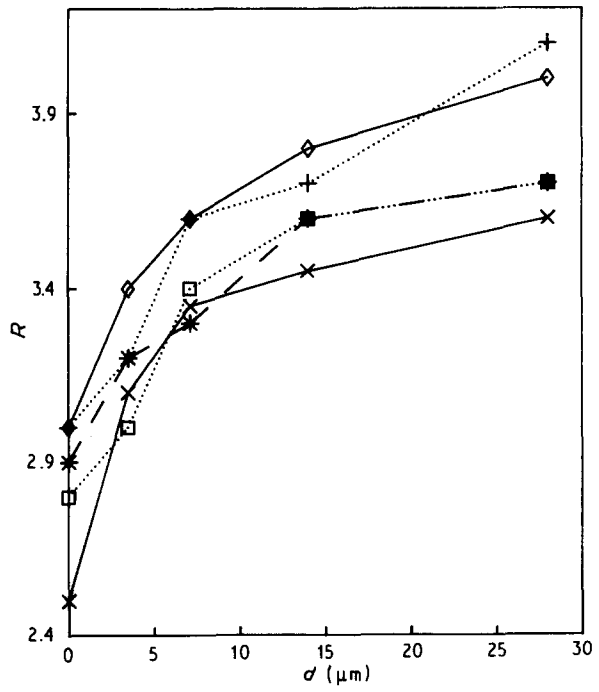

Figure 6 Peak intensity ratio $R = I_{799\ cm^{-1}} / I_{840\ cm^{-1}}$ plotted versus the distance, d, from the centre where the spectra were recorded for the microindentation obtained with loads of (+) 0.25 N, (◇) 0.50 N, (✳) 1.0 N, (□) 1.5 N and (×) 2.0 N.

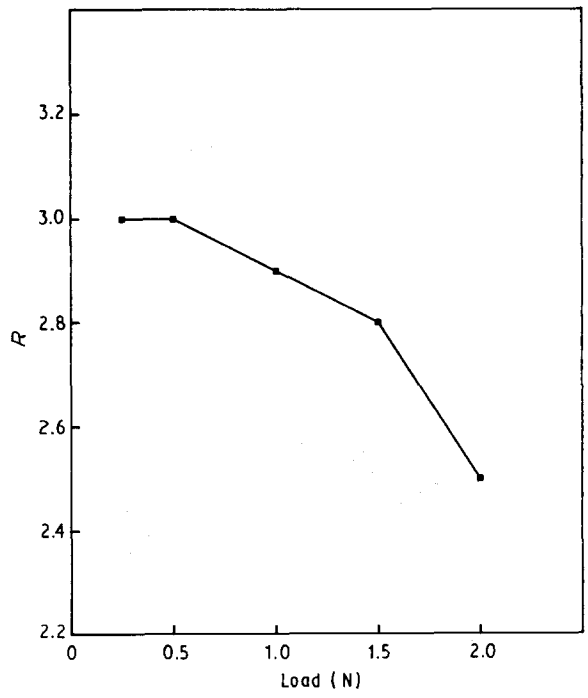

Figure 7 R plotted versus load for spectra recorded at the centre of the impression.

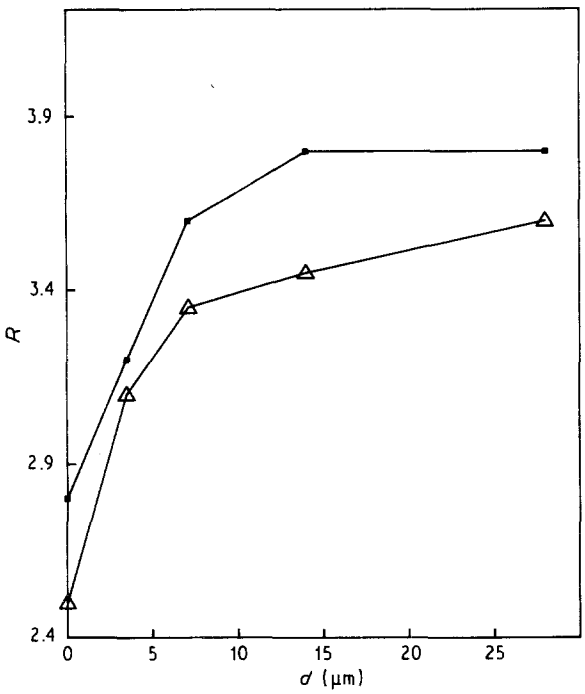

Figure 8 R plotted against d for two microindentations obtained with a load of 2 N (a) with instantaneous unload when the maximum load is reached (■) and (b) applying the load for 1 min (△).

transformation distribution along the microindentation.

The Raman spectra were also scanned along one of the diagonals at the positions A, F (0, 2.5 μm), G (0, 5 μm), H (0, 10 μm), I (0, 20 μm) for the microindentations obtained with a load of 0.5 N. The resulting plot giving R versus d is presented in Fig. 9. In addition, the plot of Fig. 6 for a load of 0.5 N is also given in Fig. 9 in order to compare the crystalline

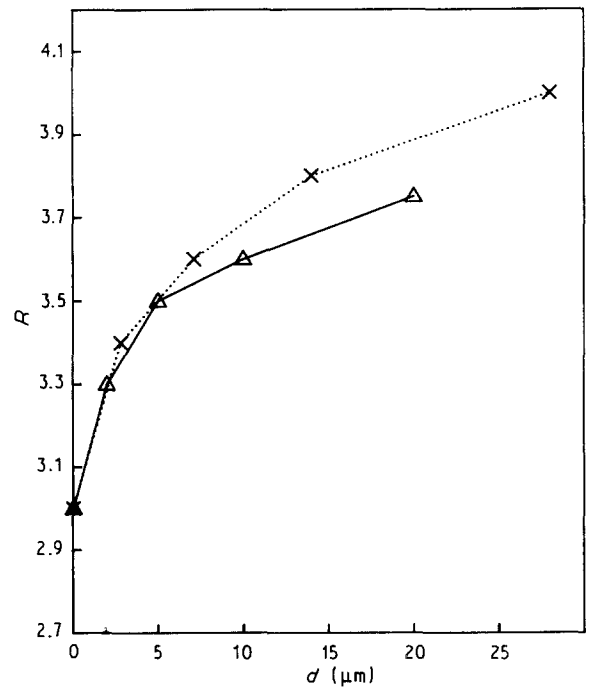

Figure 9 R plotted versus d (——) along the diagonal and (– – –) along the line of maximum gradient, for the microindentation obtained with a load of 0.5 N.

phase variation along the diagonal and along the line of maximum gradient in depth.

4. Discussion

Fig. 1 indicates that the intensity of the bands at 799 and 840 cm^{-1} is sensitive to the pressure applied to PVF_2, as the pressure is increased the intensity of the band at 840 cm^{-1} corresponding to Form I increases, whereas that of the band at 799 cm^{-1} characteristic of Form II, falls. Hence, these results are in good agreement with previous works which showed that drawing PVF_2 produces a phase transition from Form II to Form I [15, 16]. Consequently, the study of these two Raman bands of PVF_2 can be utilized for determining the variation of pressure in and around a microindentation produced in PVF_2.

Figs 4–9 show the same trend, that is the intensity ratio, R, between the 799 and 840 cm^{-1} bands increases as the position where the Raman spectra were recorded varies from the centre to the edge of the microindentation. These results reflect that the distribution of pressures inside the indentation decreases from the centre to the edge of the microindentation. These results confirm initial data obtained on poly (3,3-dimethyl oxetane) [14]. The process of microindentation follows a complex viscoelastic deformation behaviour characteristic of polymeric materials. The gradient in the pressure distribution may be explained by different characteristics of the process of microindentation in polymers. One of the possible reasons is that the degree of the elastic deflection surrounding the contact zone varies as the indentor penetrates the sample. This would result in a variation of the elastic tensions during the process of indentation, which may then affect the distribution of pressures in the contact zone. Another explanation may be that a type of work hardening occurs as the indentor is introduced in the sample. This will result in a zone of higher stress around the centre of the indentation which decreases as the position is moved up to the edge of the impression. Other effects, such as the variation of creep during the process of microindentation, may also explain such a distribution of pressures.

It may also be observed that although the trend of distribution of tensions inside the impression zone is approximately the same for microindentations obtained with different loads, the crystalline phase transformation increases as the load is augmented (see Fig. 6). The dependence of the crystalline variation on the applied load inside the microindentation could be explained by a type of work hardening as proposed above, i.e. as greater loads are applied to the indentor, the deformed region increases with compression of the material under the indentor, resulting in the hardening of the material. An increase of the work hardening of the material will then produce a higher efficiency in the crystalline phase transformation. According to such a description of the deformation process, the centre of the microindentation which corresponds to the zone of highest depth will be submitted to the greatest stress.

Fig. 8 shows that the degree of crystalline transformation increases with the duration of the applied load. This result is coherent with the viscoelastic behaviour of polymers which is time dependent. Thus, as the time of applied load is increased, the degree of work hardening also increased producing an increase in the efficiency of crystalline phase transformation.

When Figs 2 and 7 are compared, it can be observed that the degree of crystalline modification for the same pressure (if we compare the microhardness value to the pressure produced by the press machine on the PVF_2 plate), is greater for PVF_2 deformed between two flat plates than by microindentation. These features may be explained by the fact that in the case of the process of microindentation, stress relaxation can easily occur out of the permanent deformed zone, whereas in the case of a sample pressed between two plates such a relaxation can hardly take place.

4. Conclusion

This micro-Raman analysis of the microdeformation of PVF_2 by a Vickers microindentation is in excellent agreement with a previous study obtained on poly (3,3-dimethyl oxetane), that is the distribution of pressure is not constant inside the microindentation. This present work highlights new features in the process of microindentation, such as the general trend of the variation of stress in the microdeformed region for different loads and the dependence of the crystalline phase transformation on the time of indentation. This study also shows that the distribution of stresses in the microindentation in PVF_2 depends on properties such as stress relaxation and work hardening. The rapid evolution of crystalline phase transformation with the distance from the centre of the indentation is probably due to a greater work hardening in the zone close to the tip of the indentor. Such an effect increases the degree of efficiency in crystalline phase transformation in the region near the centre of the microindentation.

Acknowledgements

The authors thank the Junta de Castilla y León and CICYT under the project PA86-0198 for financial support.

References

1. F. J. BALTA-CALLEJA, J. MARTINEZ-SALAZAR and D. R. RUEDA in "Encyclopedia of Polymer Science and Engineering" Vol. 7, edited by H. F. Mark, N. M. Bikales, C. G. Overberger and G, Menges, (Wiley, New York, 1987) p. 614.
2. F. J. BALTA-CALLEJA, J. MARTINEZ-SALAZAR, H. CACKOVIC and J. LOBODA-CACKOVIK, *J. Mater. Sci.* **16** (1981) 739.
3. F. J. BALTA CALLEJA, *Adv. Polym. Sci.* **66** (1985) 19.
4. F. J. BALTA-CALLEJA and H.-G. KILIAN, *Colloid Polym. Sci.* **266** (1988) 29.
5. V. LORENZO, J. M. PEREÑA and J. G. FATOU, *Angew. Makromol. Chem.* **172** (1989) 25.
6. J. M. PASTOR, A. GONZÁLEZ and J. A. SAJA, *J. Appl. Polym. Sci.* **38** (1989) 2283.
7. B. MARTIN, J. M. PEREÑA, J. M. PASTOR and J. A. SAJA, *J. Mater. Sci. Lett.* **5** (1986) 1027.
8. F. ANIA, J. MARTINEZ-SALAZAR and F. J. BALTA-CALLEJA, *ibid.* **24** (1989) 2934.
9. J. M. PEREÑA, B. MARTIN and J. M. PASTOR, *J. Mater. Sci. Lett.* **8** (1989) 349.
10. C. C. GONZALEZ, J. M. PEREÑA, A. BELLO, B. MARTIN, J. C. MERINO and J. M. PASTOR, *ibid.* **8** (1989) 1418.
11. L. E. SAMUELS, in "Microindentation Techniques in Materials Science and Engineering", edited by P. J. Blau and B. R. Lawn (ASTM, Philadelphia, PA, 1986) p. 5.
12. J. L. LOUBET, J. M. GEORGES and G. MEILLE, *ibid.*, p. 72.
13. D. TABOR, *ibid.*, p. 129.
14. T. JAWHARI, J. C. MERINO and J. M. PASTOR, *J. Mater Sci.* **27** (1992) 2231.
15. K. TASHIRO and M.KOBAYASHI, *Phase Trans.* **18** (1989) 213.
16. K. TASHIRO and H. TADAKORO, in "Encyclopedia of Polymer Science and Engineering", edited by H. F. Mark, N. M. Bikales, C. G. Overberger and G. Menges, Suppl. Vol., (Wiley Interscience, New York, 1989) p. 213.
17. F. G. BOERIO and J. L. KOENIG, *J. Polym. Sci. A-2* **7** (1969) 1489.
18. *Idem, ibid.* **9** (1971) 1317.
19. G. L. CESSAC and J. G. CURRO, *J. Polym. Sci. Polym. Phys.* **12** (1974) 695.
20. K. TASHIRO, M. KOBAYASHI and H. TADOKORO, *Macromol.* **14** (1981) 1758.

Received 6 February
and accepted 16 April 1991